Astronomy & Astrophysics

Stellar tracers of the Cygnus Arm[*]

II. A young open cluster in Camelopardalis OB3

I. Negueruela and A. Marco

Departamento de Física, Ingeniería de Sistemas y Teoría de la Señal, Escuela Politécnica Superior, Universidad of Alicante, Apdo. 99, 03080 Alicante, Spain
e-mail: ignacio@dfists.ua.es

ABSTRACT

Context. Cam OB3 is the only defined OB association believed to belong to the outer Galactic arm or Cygnus arm. Very few members have been observed and the distance modulus to the association is not well known.

Aims. We attempt a more complete description of the population of Cam OB3 and a better determination of its distance modulus.

Methods. We present *uvby* photometry of the area surrounding the O-type stars BD +56°864 and LS I +57°138, finding a clear sequence of the early-type stars that define an uncatalogued open cluster, which we call Alicante 1. We also present spectroscopy of stars in this cluster and the surrounding association.

Results. From the spectral types for 18 very likely members of the association and *UBV* photometry found in the literature, we derive individual reddenings, finding a extinction law close to standard and an average distance modulus $DM = 13.0 \pm 0.4$. This value is in excellent agreement with the distance modulus to the new cluster Alicante 1 found by fitting the photometric sequence to the ZAMS. In spite of the presence of several O-type stars, Alicante 1 is a very sparsely populated open cluster, with an almost total absence of early B-type stars.

Conclusions. Our results definitely confirm that Cam OB3 is located on the Cygnus arm and identify the first open cluster known to belong to the association.

Key words. stars: early-type – stars: distances – Galaxy: structure – open clusters and associations: individual: Cam OB3 – stars: Hertzsprung-Russell (HR) and C-M diagrams – techniques: photometric

1. Introduction

The structure of the Milky Way is still the subject of controversy. While many authors have argued for a four-armed Galaxy (e.g., Vallée 2005; Russeil 2003), two-armed models have also remained popular (e.g., Fernández et al. 2001). Recent results based on star counts from the GLIMPSE survey (Benjamin et al. 2005) favour a two-armed Galaxy, with the Scutum-Crux (i.e., the second arm towards the Galactic centre from the position of the Sun or −II) and the Perseus (the first arm towards the outside from the position of the Sun or +I) arms as main features. This is a surprising result, as previous authors had considered the Sagittarius-Carina (−I) and the Norma (−III or internal) arms as the main features (e.g., Georgelin & Georgelin 1976).

Unfortunately, our view from the Galactic periphery is not the most adequate for studying Galactic structure. For example, the Perseus arm, now believed to be a major spiral feature, cannot be traced beyond Galactic longitude $l \approx 140°$, though some tracers seem to be found around $l \approx 180°$. This could reflect a flocculent morphology for the outer Milky Way (e.g., Quillen 2002).

Beyond the Perseus arm, molecular clouds definitely delineating an outer arm, generally referred to as the Cygnus arm, are readily visible in CO surveys all over the first Galactic quadrant (Dame et al. 2001). In most models, the Cygnus arm is

assumed to be the continuation of the Norma arm. In a previous paper (Negueruela & Marco 2003, henceforth Paper I), we presented spectroscopy for several stars that could belong to the Cygnus arm. Tracers were particularly reliable in the region $l \approx 140°–180°$, where the Perseus arm is not present along the line of sight. Several stars around $l = 147°$ were assumed to belong to the association Cam OB3.

The existence of Cam OB3 has sometimes been considered doubtful, as the density of members is not very high and no previously catalogued open clusters are contained. Using data in the literature for 6 likely members, Humphreys (1978) centred it at ($l = 147°$, $b = +3.0$) and derived $DM = 12.6$. Haug (1970) obtained *UBV* photometry of a larger number of OB stars in the first volume of the Luminous Star catalogue and, based on estimated distances, considered the existence of Cam OB3 certain. In Paper I, we obtained spectroscopy for 10 likely members and found that their calculated distance moduli concentrated very tightly around $DM = 13.0$. This *DM* is one and a half magnitudes higher than those to Per OB1 and Cas OB6, the tracers of the Perseus arm closest in the sky, implying that Cam OB3 is clearly too far away to be on the Perseus arm.

During this work, we noticed that sky images of the area between the O-type stars BD +56°864 (O6 Vnn, double-lined spectroscopic binary) and LS I +57°138 (O7 V) showed a very high concentration of moderately bright stars. In this paper, we present photometry of the area, clearly showing the presence of an early-type star sequence identifiable as a small open cluster. We also present a rather larger spectroscopic sample of possible

---

Table 1. Log of the photometric observations taken at the 2.2-m in October 2002, with all times in seconds.

Alicante 1	RA = 03h59m18.29s		Dec = +57°14′13.7″
	(J2000)		(J2000)
Filter	Long times	Intermediate times	Short times
u	1400	100	5
v	400	40	2
b	400	40	2
y	400	40	2

Table 2. Mean catalogue minus transformed values (D) for the standard stars and their standard deviations in V, $(b − y)$ and c_1.

	V	$(b − y)$	c_1
D	0.00	0.00	0.00
σ	0.02	0.03	0.03

members of Cam OB3, allowing us a much better definition of the association.
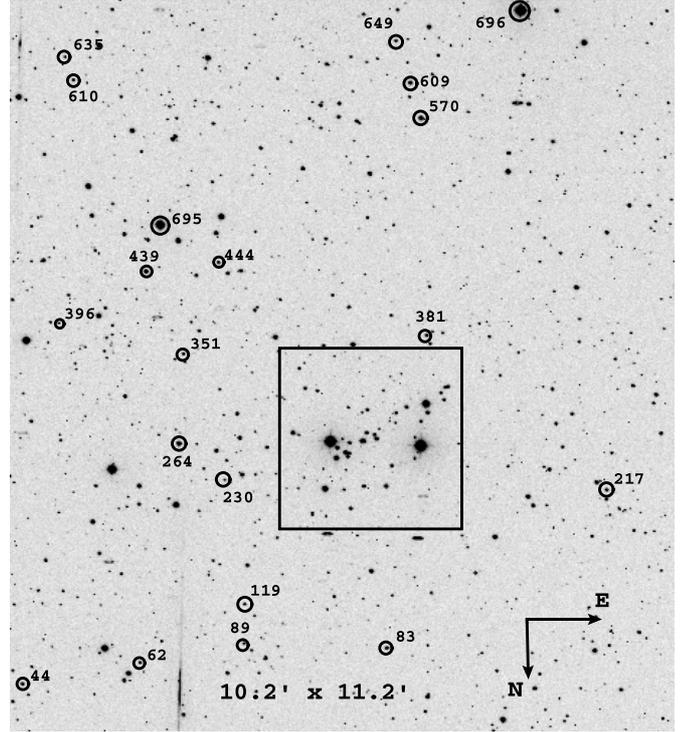
2. Observations and data

2.1. Photometry

We obtained Strömgren *uvby* photometry of the region around the star BD +56°864 using BUSCA attached to the 2.2-m telescope at the Calar Alto Observatory (Almeria, Spain) on the nights of 24−26 October 2002.

The instrument splits the light into 4 channels, each equipped with a CCD camera, which can take images at the same time in different filters. We used the 3 bluer channels to obtain images with the *uvby* filters. Each camera covers a field of view of 12′ × 12′ and has a pixel scale of 0.″176. Images from the area were taken using 3 series of different exposure times to obtain accurate photometry for a magnitude range. These exposure times are given in Table 1.

The reduction of the images was done with IRAF[1] routines for the bias and flat-field corrections. The photometry was obtained by point-spread function (PSF) fitting using the DAOPHOT package (Stetson 1987) provided by IRAF. The apertures were the same for standard and target stars. To construct the PSF empirically, we manually selected bright stars (typically 25 stars) over the whole field as good candidates for PSF stars. Once we had the list of candidate PSF stars, we determined an initial PSF by fitting the best function among the 5 options available in the PSF routine inside DAOPHOT. We chose the PSF to be variable in order 2 across the frame to take the systematic pattern of PSF variability with position on the chip into account.

We selected secondary standard stars from Marco & Bernabeu (2001). We performed atmospheric extinction corrections and solved the transformation equations following the procedure described in Marco & Bernabeu (2001). The precision of the photometry was calculated as the dispersion of the mean of the difference (transformed value − catalogue value). The values for this run are given in Table 2.

In Fig. 1, we show the area observed. Likely members of the cluster are numbered. As this is a newly discovered cluster, we

---

[1] IRAF is distributed by the National Optical Astronomy Observatories, which are operated by the Association of Universities for Research in Astronomy, Inc., under cooperative agreement with the National Science Foundation.

Fig. 1. Finding chart for stars belonging to the blue sequence in Fig. 4 (possible cluster members). *XY* positions are listed in Table 7, where they are correlated to RA and Dec. The origin of coordinates is located in the bottom left corner of the image. The area inside the square is displayed in the following figure. North is down and east to the right. This is a *y*-band image taken with BUSCA. The field of view is 10.′2 × 11.′2 and the central coordinates are RA = 03 h 59 m 19 s and Dec = +57°11′53″ in epoch J2000.

use our own numbering system. In Fig. 2, we zoom in on the area of the image marked with a square, which contains the majority of cluster members. In Table 7, we give *X* and *Y* positions for stars in Figs. 1 and 2, together with their identification in the 2MASS catalogue an their coordinates (right ascension, RA, and declination, Dec) in epoch J2000. In Table 8, we give the values of V, $(b − y)$ and c_1 for these stars.

2.2. Spectroscopy

Observations of several stars in Cam OB3, including the three O-type stars likely connected with the new cluster, were presented in Paper I. These spectra were obtained with the *Aurélie* spectrograph on the 1.52-m telescope at the Observatoire de Haute Provence (OHP) during runs on 18−22 January 2002 and 25−28 February 2002 (see Paper I for details). The spectra of the three O-type stars in the cluster area are shown in Fig. 3.
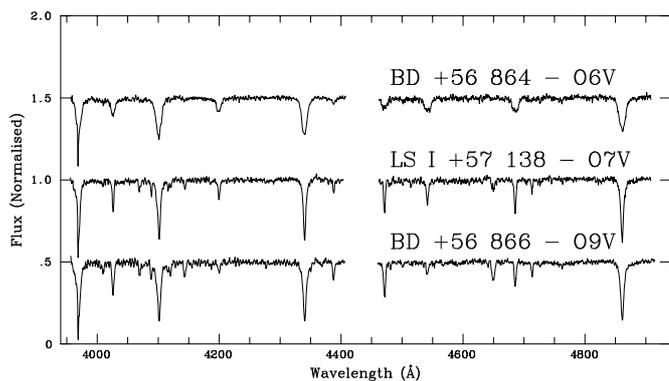
A few objects, which were not observed over the whole 3960−4910 Å range, were not included in Paper I, as their spectral types were not certain, in most cases because the spectra clearly showed lines corresponding to two stars. These observations are listed in Table 3.

Other spectra of these and other stars in Cam OB3 were obtained with the Intermediate Dispersion Spectrograph (IDS) at the 2.5-m Isaac Newton Telescope (INT) in La Palma (Spain) during a run on 23−26 July 2002. The instrument was equipped with the 235-mm camera, the R1200Y grating, and the Tek#5 CCD. This configuration gives a dispersion of
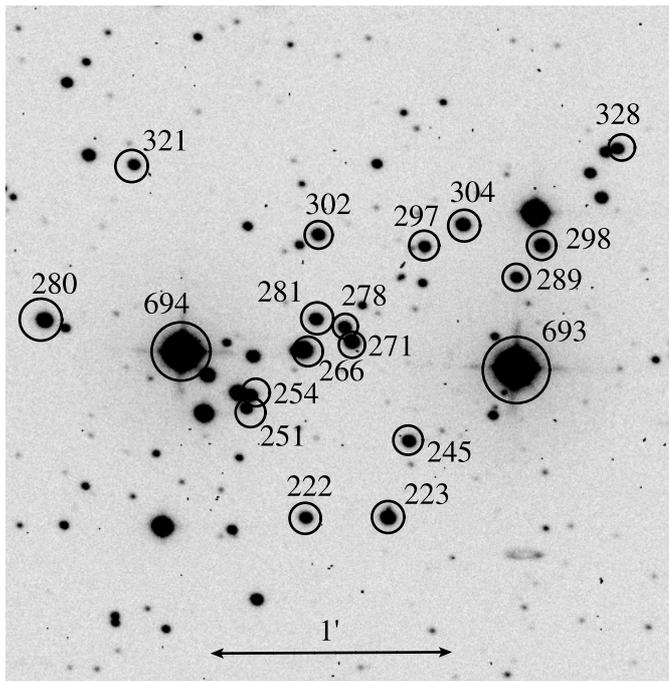
Fig. 2. Finding chart for likely cluster members in the central concentration. *XY* positions are listed in Table 7, where they are correlated to RA and Dec. The origin of coordinates is located in the bottom left corner of Fig. 1.

Fig. 3. OHP 1.52-m spectra of the three O-type stars in the area that we investigated. The identifications in Figs. 1 and 2 are BD +56°864 = #693, LS I +57°137 = #695 and BD +56°866 = #696. The small gap around $\lambda = 4420$ Å indicates the division between the two poses. Details of the observations are given in Paper I.

~0.8 Å/pixel over the 4050−4900 Å range. The complete log of these observations is given in Table 4.

Finally, spectra of possible members of the new cluster were obtained during different runs. Some were observed with the INT on 25−28 October 2002. The instrument was equipped with the 235-mm camera and the EEV #10 CCD. We used the R1200B grating for the brightest members (covering 3900−5200 Å) and the R400V grating for faint stars (covering 3500−7200 Å). Other members were observed on 29 August 2008 with the 2.6-m Nordic Optical Telescope (La Palma) and ALFOSC. We used grism #14 to cover the 3900−6800 Å range. Some of these spectra are shown in Figs. 7 and 8.

All the spectroscopic data have been reduced with the *Starlink* packages CCDPACK (Draper et al. 2000) and FIGARO

Table 3. Observations from the OHP 1.52-m telescope that were not included in Paper I.

Name	Date	Exposure time (s)	Wavelength range
HD 237204	28/02/02	900	3960−4410 Å
BD +55°837	25/02/02	1500	4460−4910 Å
BD +55°838	25/02/02	1500	4460−4910 Å
LS I +57°137	21/01/02	1800	4460−4910 Å
LS V +56°59	20/01/02	1800	3960−4410 Å

Table 4. Possible members of Cam OB3 observed from the INT in July 2002.

| LS number	Other name	Date	Exposure time (s)
I +56°90	–	26/07/02	800
I +56°92	–	23/07/02	450
I +56°94	–	25/07/02	500
I +56°98	HD 237204	26/07/02	300
I +55°53	–	26/07/02	800
I +55°54	–	25/07/02	500
I +55°55	BD +55°837	23/07/02	300
I +55°57	–	26/07/02	900
I +55°58	BD +55°838	23/07/02	300
I +55°47	–	25/07/02	900
V +56°59	–	25/07/02	400
I +57°136	–	25/07/02	600
I +57°137	–	26/07/02	720
I +57°140	–	26/07/02	500

(Shortridge et al. 1997) and analysed using FIGARO and DIPSO (Howarth et al. 1997).

3. Results

3.1. Photometry

We start by plotting the $V/(b - y)$ diagram for all stars in the field (see Fig. 4). The diagram shows evidence of different stellar populations, with at least two well-defined sequences. To the left of the diagram, there is a clear sequence with bluer colours, $(b - y) \lesssim 0.5$. Catalogued OB stars lie at the top of this sequence, so it seems sensible to assume that this sequence corresponds to an associated population. To check this hypothesis, we selected all the stars belonging to this sequence and plot their $V - c_1$ diagram (see Fig. 5). The stars also form a clear sequence in this diagram, with colours typical of reddened early type stars. Stars belonging to the sequence are marked in Figs. 1 and 2. It is obvious that the vast majority of the stars in the sequence are grouped together in a small area surrounding the two mid O-type stars. In view of the spatial concentration of the photometric sequence, we conclude that these stars are members of a previously uncatalogued open cluster in this region, which we provisionally call Alicante 1.

Our procedure may leave out some cluster members, but guarantees that most candidates selected are cluster members. The sequence shows little spread in $E(b - y)$ (see following section), making it unlikely that main-sequence members with higher reddenings are left out. Moreover, Zdanavičius et al. (2005) argue that most of the reddening in this direction originates close to the Sun. The young age of Alicante 1 (see Sect. 4.1) precludes the existence of evolved members. Pre-main-sequence (PMS) members are likely to exist, and our
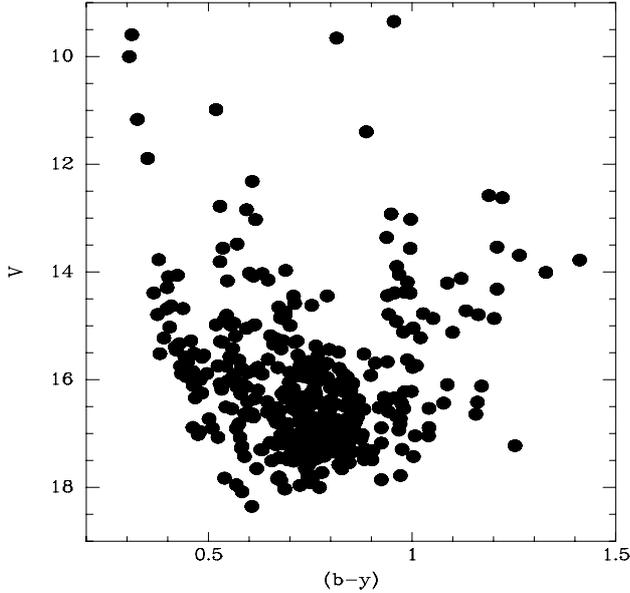
Fig. 4. $V/(b-y)$ diagram for all stars in the field. We identify the bluer sequence as the new cluster Alicante 1.
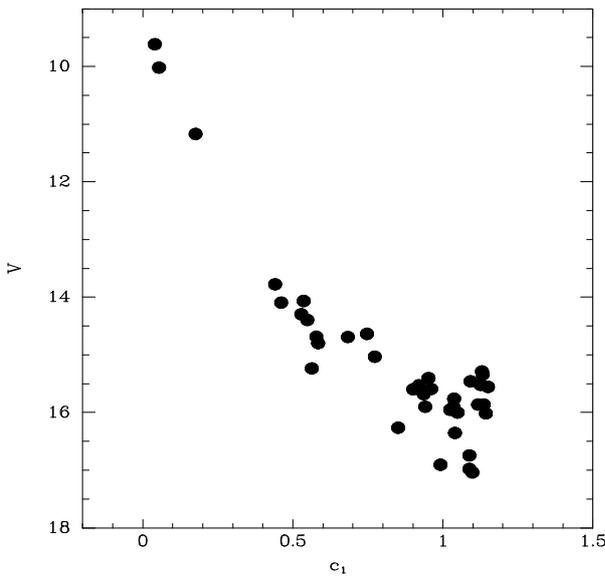
Fig. 5. V/c_1 diagram for the stars stars identified as possible cluster members in Fig. 4.

selection procedure is likely to leave out most of them. Finding these PMS objects out from photometry alone is very difficult, as they will not have typical colours, and the cluster is sparse and mixed with large foreground and background populations. A search for emission-line objects may produce a sample of this population.

Our selection of candidates leaves 38 stars as possible members of the new cluster Alicante 1. Now we can use the photometric analysis to determine its distance. First, we need to deredden the values for V, $(b-y)$ and c_1. For this purpose, we calculate individual reddenings following the procedure described by Crawford et al. (1970) for B-type stars: we use the observed c_1 to predict the first approximation to $(b-y)_0$ with the expression $(b-y)_0 = -0.116 + 0.097c_1$. Then we calculate $E(b-y) = (b-y) - (b-y)_0$ and use $E(c_1) = 0.2E(b-y)$ to correct c_1 for reddening $c_0 = c_1 - E(c_1)$. The intrinsic colour $(b-y)_0$ is

now calculated by replacing c_1 with c_0 in the above equation for $(b-y)_0$. Three iterations are enough to reach convergence in the process. The final values of $E(b-y)$, $E(c_1)$ and c_0 are given in Table 8. We note that this procedure assumes that the reddening law is the average for nearby stars. We will see in Sect. 3.3 that this assumption is justified.

The reddening is quite constant across the cluster. The average value is $E(b-y) = 0.48$ for 38 possible members, with a dispersion of only $\sigma = 0.03$, comparable to the precision of the $(b-y)$ colour in our photometry. No star deviates by more than 2σ from the average value, which corresponds to $E(B-V) = 0.67$.

Next, we plot the $V_0/(b-y)_0$ and V_0/c_0 diagrams (see Fig. 6) and calculate the distance modulus DM that gives the best fit to the ZAMS (Perry et al. 1987) in both diagrams. The best fit for the distance modulus is $DM = 13.0 \pm 0.2$, using the sequence of late B and early-A stars. In the V_0/c_0 diagram, it is clear that the three brightest members are displaced vertically from their expected positions. This is a suggestion of a binary nature, and we see in Sect. 3.2.1 that two of the three are spectroscopic binaries. Their position in the diagram is compatible with the same DM if this is taken into account. In Table 8, we list the dereddened photometric indices and the derived values for absolute magnitudes calculated as $M_V = V_0 - 13.0$.
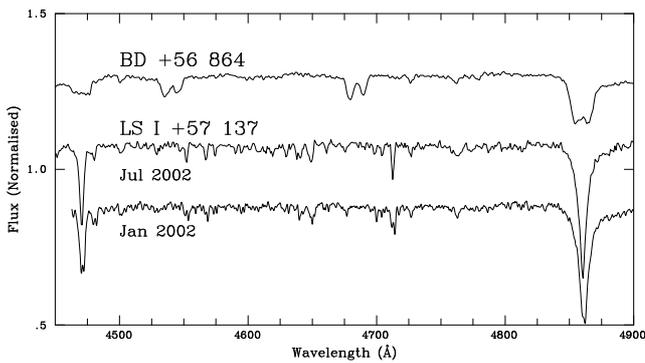
3.2. Spectroscopy

3.2.1. Cluster members

The brightest member of Alicante 1 is BD +56°864 (#693). Several spectra of this object show double lines (see Fig. 7). The two components have similar spectral types around O6 V. This system is a short period binary and will be studied in detail in forthcoming work. Double lines are also evident in the OHP spectrum of LS I +57°137 (#695). The secondary shows weaker metallic lines and therefore appears to be slightly later than the primary. The INT spectrum can be classified as B1.5 V, but, given the double lines, this may be a combination of a ~B1 V and a ~B2 V star.

The expected absolute magnitude of an O6 V star is $M_V = -4.9$ (Martins et al. 2005), so the observed $M_V = -5.4$ of BD +56°864 is compatible with the presence of a secondary almost as bright as the primary. The expected magnitude of a B1 V star is $M_V = -3.2$, and again the observed $M_V = -3.7$ of LSI +57°137 is compatible with the presence of a bright secondary. The spectrum of LS I +57°138 (#694) (O7 V), the second brightest member, does not show any evidence of a secondary component (see Fig. 3). The observed $M_V = -5.0$ is also a bit too high for a single star, but within the expected dispersion of the calibration ($M_V = -4.6$ according to Martins et al. 2005).

To the south of the field lies BD +56°866. Though this star is marked in Fig. 1 as #696, it is too close to the edge of the chip, and we could not obtain its photometry. However, its published photometry clearly shows it to be a member of Cam OB3 (see Table 5), so it is almost certainly a cluster member. The $V/(b-y)$ diagram (Fig. 4) shows a star with $V \approx 12$ that seems to belong to the cluster sequence, but is not present in Fig. 5. This object was very close to the edge of the chip in the short u exposure, and we have no c_1 index for it. It is identified as GSC 03725-00486, and its 2MASS colours show it to be an early-type star, though its $(J-K_S)$ is smaller than those of cluster members. We took a spectrum of this object, which turns out to be an A giant, hence not a cluster member.
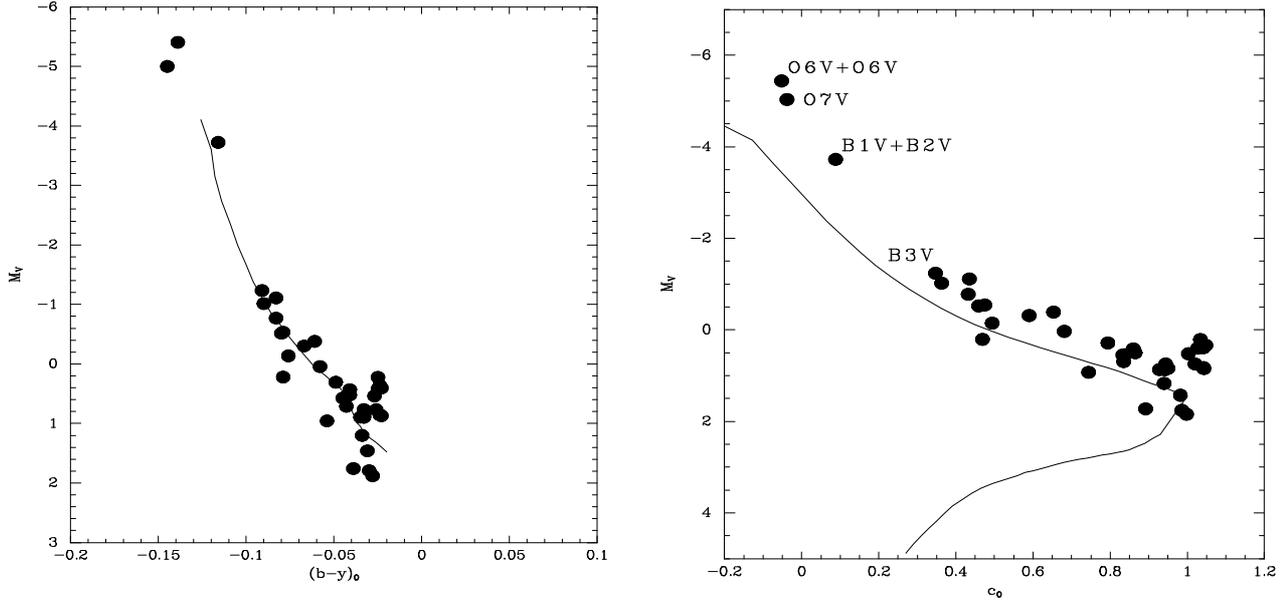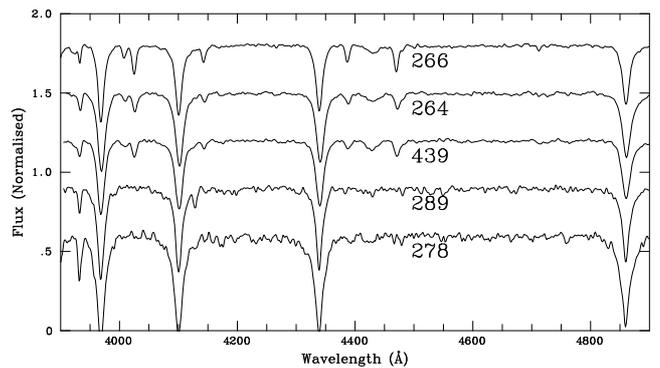
Fig. 6. *Left*: dereddened $M_V/(b-y)_0$ diagram for cluster members. *Right*: dereddened M_V/c_0 diagram for members. The spectral types for the brightest members are indicated. In both panels, the line represents the ZAMS from Perry et al. (1987).

Fig. 7. Spectra of two of the brightest members of Alicante 1 showing that they are double-lined spectroscopic binaries. BD +56°864, originally classified as O6 Vnn, has two similar components. In the case of LS I +57°137, the spectrum from 2002 July shows a single component of spectral type B1.5 V. However, the 2002 January spectrum clearly shows double He I and Mg I 4481 Å lines and weak second components in other metallic lines.

Fig. 8. Spectra of some cluster members. Stars #264, #266, and #439 are the brightest members in the photometric sequence after the catalogued OB stars, Stars #289 and #278 are fainter members observed by chance. See text for the spectral classifications.

Figure 8 shows the spectra of other likely members. The brightest non-catalogued member, #266, has spectral type B3 V. The next brightest stars, #264 and #439, have spectral types B4−B5 V, in very good agreement with their positions in the photometric diagrams. Other stars observed by chance are #289 and #278. Star #289 is located in the cluster core. It has weak Ca II 3933 Å, compatible with the purely interstellar line seen in the B-type stars. The prominent Si II 4128 Å doublet then suggests that this is a chemically peculiar Bp (Si) star. The spectral type is ~B9, and the object is likely to be a Bp member. Star #278 is also in the cluster core. It has a spectral type around A1 III−IV. As its reddening is typical of cluster members and its position in the M_V/c_0 diagram is compatible with the same distance modulus as the rest of the cluster, it may only be a chance alignment of a nearby unrelated star or a PMS cluster member. PMS stars without emission lines have been identified in clusters with low background contamination, such as NGC 1893 (Negueruela et al. 2007). As a matter of fact, #278 is part of

a small clump of objects with $c_0 \approx 1.0$, lying slightly above the rest of the sequence (Fig. 6), and this discussion may apply to all of them.

3.2.2. Other members of Cam OB3

For all the candidate members of Cam OB3, we derive spectral types following the prescriptions described in Paper I. The resulting spectral types are listed in Table 5. We use this information to derive the reddening and distance to the stars in the next section. In the OHP spectrum, LS V +56°59 clearly appears as a double-lined spectroscopic binary. The H I and He I lines of the secondary spectrum are weaker than those of the primary, while the metallic lines appear similar in strength. HD 237204 is also likely to be a double-lined spectroscopic binary, as all metallic lines appear very broad in the two available spectra. Rubin (1965), however, did not detect any variability in its radial velocity. The lines of LS I +57°140 are also broad and asymmetric, but the presence of a secondary spectrum is not certain.

Table 5. Candidate members of Cam OB3, with their spectral types, photometry from the literature, and derived parameters.

LS number	l	b	Spectral type	V	Ref.[1]	R	$E(B-V)$	m_V	DM
I +55°47	143°.5	−1°.5	O9 III	11.25	h	2.88 ± 0.08	1.35 ± 0.03	7.34 ± 0.04	12.6
I +56°90	145°.9	+1°.9	B1.5 V(+)	12.24	h	2.74 ± 0.12	0.81 ± 0.03	9.98 ± 0.04	12.8
I +57°136	146°.0	+2°.9	O8.5 V	10.88	h	2.92 ± 0.15	0.66 ± 0.03	8.90 ± 0.04	13.1
I +56°92	146°.0	+2°.4	B5 IIe	10.26	h	3.38 ± 0.14	0.86 ± 0.03	7.31 ± 0.04	12.7
I +57°140	146°.1	+3°.5	B0.2 IV(+)	11.02	h	2.91 ± 0.17	0.60 ± 0.03	9.22 ± 0.04	13.7
I +56°94	146°.2	+2°.8	B1.5 IV	11.77	h	3.00 ± 0.25	0.46 ± 0.03	10.37 ± 0.04	13.7
I +57°137	146°.3	+3°.1	B1.5 V+	11.23	h	2.90 ± 0.20	0.52 ± 0.03	9.66 ± 0.04	12.5
I +57°138	146°.3	+3°.1	O7 V	10.09	h	3.20 ± 0.19	0.56 ± 0.02	8.27 ± 0.04	12.9
I +57°139	146°.3	+3°.1	O6 V+	9.67	h	2.74 ± 0.18	0.56 ± 0.02	8.14 ± 0.04	13.1
I +56°97	146°.4	+3°.1	O9 V	10.33	h	2.94 ± 0.17	0.64 ± 0.03	8.42 ± 0.04	12.5
I +56°98	146°.6	+3°.0	B0.5 V+	9.17	h	2.86 ± 0.19	0.54 ± 0.03	7.59 ± 0.04	11.1
I +55°54	146°.9	+1°.8	B0.2 IV	11.77	h	2.92 ± 0.12	0.85 ± 0.03	9.26 ± 0.04	13.8
I +55°53	147°.7	+1°.5	B3 III*	11.83	h	3.11 ± 0.11	1.00 ± 0.03	8.69 ± 0.04	11.7
I +55°55	147°.0	+2°.0	BC1.5 Ib	9.59	h	2.97 ± 0.13	0.88 ± 0.03	6.94 ± 0.04	12.7
I +56°99	147°.1	+3°.0	O9.5 Iab	9.00	h	3.13 ± 0.14	0.74 ± 0.02	6.64 ± 0.04	12.9
V +56°56	147°.4	+3°.9	B5 Ia	7.99	hi	3.51 ± 0.19	0.64 ± 0.03	5.73 ± 0.04	12.9
I +55°57	147°.5	+1°.8	B1 IV*	12.19	h	2.96 ± 0.14	0.78 ± 0.03	9.81 ± 0.04	13.6
I +55°58	147°.6	+1°.9	B2.5 Iab	9.29	h	2.98 ± 0.11	1.00 ± 0.03	6.28 ± 0.04	12.8
V +55°11	147°.6	+2°.7	B6 Ia	8.72	hi	3.15 ± 0.14	0.84 ± 0.03	6.04 ± 0.04	13.0
V +56°59	149°.7	+5°.3	B1 V+	10.92*	−	−	−	−	12.6
V +56°60	149°.8	+5°.7	B2.5 III	11.51*	−	−	−	−	13.7
V +53°22	151°.6	+2°.9	B0 Ia	9.32	hi	3.21 ± 0.13	0.90 ± 0.03	6.39 ± 0.04	13.0

[1] The references for the *UBV* photometry are (h) Haug (1970) or (hi) Hiltner (1956). The *JHK$_S$* photometry is from 2MASS. Two stars have no accurate *UBV* photometry and their distance moduli are estimates (see Paper I).

3.3. Reddening and distance to Cam OB3

To determine the reddening and distance to the isolated stars, we used *UBV* photometry from the literature. As in Paper I, we took Haug (1970) as our prime source of photometry, supplemented by Hiltner (1956). Both authors use the same photometric system. In addition, we collected *JHK$_S$* photometry from the 2MASS catalogue (Skrutskie et al. 2006). The photometry was used as input for the χ^2 code for parametrised modelling and characterisation of the photometry and spectroscopy CHORIZOS implemented by Maíz-Apellániz (2004). This code generates synthetic photometry from a stellar model and convolves it with extinction laws from Cardelli et al. (1989). A fit to the real photometric data determines the values of R and $E(B-V)$ that would most likely result in the observed photometry for a star with the given spectrum. In Table 5, we list the spectral types derived for all candidate members of Cam OB3, the photometry collected from the literature and the values obtained for R and $E(B-V)$. We consider all the candidate members from Paper I and the objects listed in Table 4.

The results of the fits with CHORIZOS favour values of R very close to the standard value $R = 3.1$. There are few exceptions. LS I +56°92 is an emission-line object (cf. Negueruela 2004) and the high value of R found reflects the presence of a circumstellar excess. The value adopted for the *DM* of this object is an approximation assuming standard reddening and no excess in $E(B-V)$ (formally, this should be taken as a lower limit, but is unlikely to differ much from the actual value). The B5 Ia supergiant HD 25914 (LS V +56°56) also has a very high value for R, suggesting a circumstellar excess as well. This is a known variable (GQ Cam), likely to be a very luminous star. Leaving aside these two objects, we have an average $R = 2.97 ± 0.14$ (where the error represents the standard deviation of the sample). This value is compatible within errors with the standard value. Based on a photometric study of stars in the area, Zdanavičius et al. (2005) conclude that $R = 2.9$, in very good agreement with

Table 6. Absolute magnitude calibration used here.

	V	IV	III	II	Ib	Ia
O6	−4.9	−	−5.7	−	−	−6.4
O7	−4.6	−	−5.5	−	−	−6.5
O8	−4.3	−	−5.4	−	−	−6.5
O9	−4.1	−	−5.3	−	−6.0	−6.5
O9.5/7	−3.9	−	−5.2	−	−6.0	−6.6
B0	−3.8	−4.5	−5.1	−5.8	−6.0	−6.6
B0.2	−3.8	−4.5	−5.1	−5.6	−6.0	−6.7
B0.5	−3.5	−4.2	−5.0	−5.5	−6.0	−6.9
B0.7	−3.5	−4.2	−4.8	−5.3	−6.0	−7.0
B1	−3.2	−3.8	−4.3	−5.1	−6.0	−7.0
B1.5	−2.8	−3.3	−3.9	−5.0	−5.8	−7.2
B2	−2.5	−3.1	−3.7	−4.8	−5.8	−7.4
B2.5	−2.0	−3.1	−3.5	−4.8	−5.8	−7.4
B3	−1.6	−2.5	−3.0	−4.7	−5.8	−7.2

our value, and that extinction is caused mostly by material at <1.5 kpc from the Sun. This result justifies the assumption of standard reddening used when dereddening the Strömgren photometry in Sect. 3.1. We note a tendency for double-lined stars to give lower values of R, though there are too few such systems to know if this is a real trend.

With these values, we calculated the distance modulus to each object. Since the publication of Paper I, several works have advocated a reduction in the temperature scale and absolute magnitude scale of O-type stars. Because of this, we used the absolute magnitude scale of Martins et al. (2005) rather than the one used in Paper I. For B spectral types, the calibration of Humphreys & McElroy (1984) was used. In the B0−B1 interval, the calibrations are not consistent, and an interpolation has been made, resulting in the calibration given in Table 6. For the two luminosity class Iab supergiants in the sample, we adopt $M_V = −6.3$ for LS I +56°99 (=HD 237211, O9.5 Iab) and

Table 7. Coordinates (*XY*) in the map (Fig. 1) of likely members of Alicante 1 with *ubvy* photometry, including 2MASS identification for these stars and their coordinates.

Number	RA (J2000)	Dec (J2000)	Name (2MASS)	X (Pixels)	Y (Pixels)
695*	03 58 46.53	+57 10 43.6	059.693873+57.178764	414.93	1411.15
266	03 59 11.36	+57 14 10.5	059.797345+57.236237	975.86	808.75
264	03 58 49.39	+57 14 17.2	059.705783+57.238117	466.86	801.75
570	03 59 17.33	+57 08 52.9	059.822194+57.148026	1135.31	1708.00
439	03 58 44.97	+57 11 29.6	059.687384+57.191555	376.07	1280.98
280	03 59 03.00	+57 14 04.2	059.762506+57.234509	782.23	831.13
609	03 59 15.96	+57 08 18.4	059.816485+57.138458	1106.08	1806.73
271	03 59 40.68	+57 14 52.1	059.919501+57.247795	1012.12	814.95
223	03 59 14.29	+57 14 54.2	059.809535+57.248375	1039.09	682.36
298	03 59 19.05	+57 13 41.0	059.829361+57.228069	1154.34	887.31
304	03 59 16.47	+57 13 36.1	059.818637+57.226681	1095.23	903.19
44	03 58 31.32	+57 18 16.2	059.630503+57.304493	34.41	131.62
83	03 59 14.86	+57 17 32.4	059.811910+57.292332	1040.82	231.82
281	03 59 11.80	+57 14 02.1	059.799157+57.233925	985.28	831.91
245	03 59 14.89	+57 14 33.8	059.812057+57.242710	1054.73	740.04
302	03 59 11.80	+57 13 39.7	059.799169+57.227707	986.99	895.67
278	03 59 12.72	+57 14 04.1	059.803008+57.234467	1006.64	825.77
254	03 59 14.89	+57 14 33.8	059.812057+57.242710	936.50	774.56
217	03 59 40.68	+57 14 52.1	059.919501+57.247795	1648.13	672.37
381	03 59 18.66	+57 12 25.4	059.827744+57.207047	1150.71	1103.12
444	03 58 53.60	+57 11 19.3	059.723338+57.188694	576.28	1305.51
222	03 59 11.62	+57 14 54.8	059.798424+57.248566	977.58	682.26
328	03 59 21.02	+57 13 15.9	059.837604+57.221096	1210.75	960.55
251	03 59 09.61	+57 14 26.2	059.790049+57.240608	933.08	764.68
289	03 59 18.25	+57 13 49.7	059.826022+57.230476	1135.10	863.31
649	03 59 14.10	+57 07 37.4	059.808753+57.127056	1065.84	1924.29
297	03 59 15.23	+57 13 42.2	059.813468+57.228401	1066.39	886.79
321	03 59 05.77	+57 13 22.5	059.774047+57.222904	848.99	948.38
351	03 58 49.63	+57 12 49.2	059.706797+57.213665	478.45	1051.91
610	03 58 35.77	+57 08 23.5	059.649042+57.139870	175.46	1815.13
62	03 58 45.35	+57 17 52.4	059.688969+57.297894	359.40	191.55
119	03 58 57.73	+57 16 53.0	059.740534+57.281399	648.78	353.67
89	03 58 57.74	+57 17 31.5	059.740576+57.292084	646.15	244.04
635	03 58 34.70	+57 08 01.3	059.644580+57.133690	152.05	1879.19
230	03 58 54.97	+57 14 51.8	059.729049+57.247719	593.33	700.30
396	03 58 34.71	+57 12 22.2	059.644608+57.206169	135.28	1136.67
694*	03 59 07.49	+57 14 11.7	059.781192+57.236591	883.50	806.50
693*	03 59 18.30	+57 14 13.8	059.826231+57.237160	1134.50	795.50

* Catalogued stars: #693 = BD+56°864, #694 = LS I +57°138, #695 = LSI +57°137.

$M_V = -6.5$ for LS I +55°58 (=BD +55°838, B2.5 Iab). The values obtained are also listed in Table 5.

With these values, HD 237204 (LS I +56°98) is clearly a foreground object at a distance compatible with the Perseus arm. The other 19 objects give $DM = 12.9 \pm 0.5$ (1σ). LS I +55°53 has a distance modulus $>2\sigma$ shorter than the average, and its spectral type (B3 III) suggests a star significantly less massive than all the other ones. Therefore we also take it for a foreground object. Leaving out this object, we find $DM = 13.0 \pm 0.4$.

4. Discussion

We found the small cluster Alicante 1 around BD +56°864 and derived a distance modulus $DM = 13.0 \pm 0.2$. This value is identical within the errors to the average spectroscopic distance modulus to bright members of Cam OB3. In view of this, we can firmly identify Alicante 1 as the first known cluster in Cam OB3 and confirm the distance modulus to Cam OB3 as 13.0, corresponding to 4.0 kpc.

4.1. Alicante 1

As there are no evolved stars in Alicante 1, its age cannot be accurately determined. However, the presence of mid O-type stars close to the ZAMS forces it to be <4 Myr. On the other hand, the lack of any H II region associated with the stars suggests that they must have had time to disperse their maternal cloud entirely. Therefore an age of 2−3 Myr is favoured. At this age, all stars later than ~B8 (~3 $M_{\odot}$) must still be in the pre-main-sequence phase.

The HR diagram of Alicante 1 (see Fig. 6) shows an obvious deficiency of early B-type stars. Taking into account the binary nature of BD +56°864 and the very likely membership of BD +56°866, there are at least four O-type stars in the cluster, three more massive than 30 $M_{\odot}$. In contrast, the only early B-type stars are the two components of LS I +57°137. The photometric sequence only starts at B3 V and there are not many B-type members. This mass distribution is quite different from a standard IMF (Kroupa 2001). It may be argued that, in such a small cluster, small number statistics may result in large deviations from a standard value. However, it is tempting to

Table 8. Photometry of the stars with numbers in Fig. 1.

Number	V	$(b-y)$	c_1	c_0	M_V	$E(b-y)$	$E(c_1)$
695	11.171	0.325	0.176	0.088	−3.723	0.441	0.088
266	13.777	0.377	0.441	0.347	−1.235	0.468	0.094
264	14.066	0.423	0.536	0.435	−1.110	0.506	0.101
570	14.094	0.401	0.461	0.363	−1.016	0.491	0.098
439	14.295	0.398	0.528	0.432	−0.773	0.481	0.096
280	14.394	0.365	0.548	0.459	−0.518	0.445	0.089
609	14.635	0.408	0.747	0.653	−0.383	0.469	0.094
271	14.684	0.437	0.578	0.475	−0.537	0.516	0.103
223	14.689	0.397	0.683	0.590	−0.307	0.464	0.093
298	14.796	0.374	0.584	0.494	−0.140	0.450	0.090
304	15.029	0.404	0.773	0.681	0.040	0.462	0.092
44	15.232	0.390	0.563	0.469	0.215	0.469	0.094
83	15.284	0.456	1.130	1.034	0.218	0.481	0.096
281	15.339	0.428	1.132	1.042	0.399	0.451	0.090
245	15.399	0.418	0.952	0.860	0.425	0.459	0.092
302	15.454	0.420	1.092	1.003	0.532	0.447	0.089
278	15.514	0.464	1.125	1.027	0.410	0.489	0.098
254	15.523	0.380	0.920	0.835	0.705	0.423	0.085
217	15.549	0.488	1.150	1.048	0.349	0.512	0.102
381	15.585	0.441	0.961	0.865	0.513	0.482	0.096
444	15.590	0.484	0.901	0.794	0.299	0.533	0.107
222	15.674	0.448	0.936	0.838	0.559	0.492	0.098
328	15.753	0.431	1.037	0.944	0.758	0.464	0.093
251	15.853	0.461	1.117	1.020	0.759	0.487	0.097
289	15.854	0.440	1.136	1.043	0.862	0.463	0.093
649	15.891	0.496	0.941	0.833	0.564	0.541	0.108
297	15.892	0.433	1.035	0.942	0.887	0.466	0.093
321	15.943	0.444	1.024	0.928	0.885	0.479	0.096
351	15.991	0.463	1.049	0.950	0.858	0.496	0.099
610	16.005	0.479	1.143	1.042	0.842	0.503	0.101
62	16.253	0.483	0.851	0.744	0.945	0.537	0.107
119	16.343	0.467	1.040	0.940	1.189	0.501	0.100
89	16.732	0.501	1.088	0.982	1.447	0.532	0.106
635	16.893	0.461	0.992	0.892	1.745	0.500	0.100
230	16.966	0.479	1.088	0.986	1.779	0.509	0.102
396	17.026	0.474	1.098	0.998	1.866	0.502	0.100
694	10.006	0.305	0.054	−0.038	−5.012	0.450	0.115
693	9.600	0.311	0.040	−0.052	−5.418	0.450	0.100

assume that dynamical ejection from the cluster core has played a role in shaping the observed IMF. Clusters containing hard binaries with two components of similar mass may be quite effective at ejecting stars via dynamical ejections (Leonard & Duncan 1990), especially if massive stars are mainly born as part of multiple systems (Pflamm-Altenburg & Kroupa 2006). The majority of stars ejected will be B-type stars and their ejection velocity will be inversely proportional to their mass.

The presence of BD +56°866 ∼ 5′ to the south of the two other O-type stars may represent evidence in favour of ejection, though the stellar distribution in Alicante 1 may instead result from a spread of star formation in small clumps. The only other unevolved O-type star in Cam OB3 is LS I +57°136 (O8.5 V), which lies ∼20′ away from Alicante 1. At $d = 4.0$ kpc, this corresponds to a projected separation of ≈23 pc. With a typical runaway speed of 10 km s^{-1}, a star would need 2.5 Myr to cover this distance, so a hypothetical ejection of LS I +57°136 from Alicante 1 is not unreasonable. Unfortunately, there are no accurate measurements of proper motions for this star.

The region with a higher member density is moderately small, ∼2′ across, which corresponds to ≈2.3 pc at $d = 4.0$ kpc. It contains 20 possible members earlier than ∼A2. It is difficult to assess whether the stars around the core represent a halo or rather small groups that have formed in the vicinity of the small cluster.

This spatial distribution, with small concentrations of early-type stars extended over a moderately large area, is not uncommon in this area of the sky (cf. the discussion of clumps of H II regions towards the Anticentre in Moffat et al. 1979).

4.2. Cam OB3 and the Cygnus arm

The majority of the members of Cam OB3 listed in Table 5 are evolved massive stars and hence older than Alicante 1. The cluster is not the nuclear region of the association, but may simply represent the latest small star-forming region to have actively created high-mass stars. No other concentrations are obvious amongst members.

In their photometric study of this area, Zdanavičius et al. (2005) failed to find any evidence of the Perseus arm, either as an increase in extinction or a concentration of stars. The lack of intervening material allows the identification of Cygnus arm tracers. Cam OB3 is not a very massive association, but with a radial extent >100 pc and a significant number of massive stars, it is a reliable spiral tracer. Nearby, Moffat et al. (1979) estimate $DM = 13.2 \pm 0.2$ for the young open cluster Waterloo 1, at $l = 151°.4$, in very good agreement with the distance to Cam OB3. Moffat et al. (1979) also estimate distances for two small groups of young stars associated with the H II regions Sh 2-217 and Sh 2-219 (at $l \approx 159°.3$), both of which contain embedded clusters (Deharveng et al. 2003), finding $DM = 13.1 \pm 0.3$ and $DM = 13.6 \pm 0.3$, respectively. Therefore it seems that the Cygnus arm is well traced in this area (see discussion in Paper I). The young clusters observed in this area are not very massive, and there seems to be a strong tendency towards sparse groupings of massive stars, rather than compact concentrations.

5. Conclusions

Our study of Cam OB3 has resulted in 18 likely members from the Luminous Star catalogue. When their reddenings are calculated individually, they support a value of $R = 3.0$, in good agreement with the photometric determination of Zdanavičius et al. (2005). Their average distance modulus is 13.0 ± 0.4, in good agreement with previous determinations based on fewer stars.

Around the earliest members of the association, BD +56°864 (O6 V) and LS I +57°138 (O7 V), we find a concentration of B and early A stars, which clearly trace the main sequence of a small and sparse cluster. The sequence also includes the nearby LS I +57°137 (B1.5 V) and BD +56°866 (O9 V) and some other faint stars around them. We spectroscopically confirm the brightest uncatalogued members of the sequence to be B3−5 V stars. We call this uncatalogued cluster Alicante 1 and find a distance modulus of 13.0 ± 0.2 from ZAMS fitting.

These results definitely confirm the existence of Cam OB3 as an association in the Cygnus arm and allow an accurate determination of its distance as 4.0 ± 0.4 kpc.

and Sweden, in the Spanish Observatorio del Roque de los Muchachos of the Instituto de Astrofisica de Canarias. The data were taken with ALFOSC, which is owned by the Instituto de Astrofísica de Andalucía (IAA) and operated at the Nordic Optical Telescope under agreement between IAA and the NBIfAFG of the Astronomical Observatory of Copenhagen.

This research has made use of the Simbad data base, operated at CDS, Strasbourg, France. This publication makes use of data products from the Two Micron All Sky Survey, which is a joint project of the University of Massachusetts and the Infrared Processing and Analysis Center/California Institute of Technology, funded by the National Aeronautics and Space Administration and the National Science Foundation.

References

Benjamin, R. A., Churchwell, E., Babler, B. L., et al. 2005, ApJ, 630, L149
Cardelli, J. A., Clayton, G. C., & Mathis, J. S. 1989, ApJ, 345, 245
Crawford, D. L., Glaspey, J. W., & Perry, C. L. 1970, AJ, 75, 822
Dame, T. M., Hartmann, D., & Thaddeus, P. 2001, ApJ, 547, 792
Deharveng, L., Zavagno, A., Salas, L., et al. 2003, A&A, 399, 1135
Draper, P. W., Taylor, M., & Allan, A. 2000, Starlink User Note 139.12, R.A.L.
Fernández, D., Figueras, F., & Torra, J. 2001, A&A, 372, 833
Georgelin, Y. M., & Georgelin, Y. P. 1976, A&A, 49, 57
Haug, U. 1970, A&AS, 1, 35
Hiltner, W. A. 1956, ApJS, 2, 389
Howarth, I., Murray, J., Mills, D., & Berry, D. S. 1997, Starlink User Note 50.20, R.A.L.
Humphreys, R. M. 1978, ApJS, 38, 309
Humphreys, R. M., & McElroy, D. B. 1984, ApJ, 284, 565
Kroupa, P. 2001, MNRAS, 322, 231
Leonard, P. J. T., & Duncan, M. J. 1990, AJ, 99, 608
Maíz-Apellániz, J. 2004, PASP, 116, 859
Marco, A., & Bernabeu, G. 2001, A&A, 372, 477
Martins, F., Schaerer, D., & Hillier, D. J. 2005, A&A, 436, 1049
Moffat, A. F. J., Fitzgerald, M. P., & Jackson, P. D. 1979, A&AS, 38, 197
Negueruela, I. 2004, AN, 325, 380
Negueruela, I., & Marco, A. 2003, A&A, 406, 119 (Paper I)
Negueruela, I., Marco, A., Israel, G. L., & Bernabeu, G. 2007, A&A, 471, 485
Perry, C. L., Olsen, E. H., & Crawford, D. L. 1987, PASP, 99, 1184
Pflamm-Altenburg, J., & Kroupa, P. 2006, MNRAS, 373, 259
Quillen, A. C. 2002, AJ, 124, 924
Russeil, D. 2003, A&A, 397, 133
Rubin, V. C. 1965, ApJ, 142, 934
Shortridge, K., Meyerdicks, H., Currie, M., et al. 1997, Starlink User Note 86.15, R.A.L.
Skrutskie, M. F., Cutri, R. M., Stiening, R., et al. 2006, AJ, 131, 1163
Stetson, P. B. 1987, PASP, 99, 191
Vallée, J. P. 2005, AJ, 130, 569
Zdanavičius, J., Zdanavičius, K., & Straizys, V. 2005, BaltA, 14, 31